A Computer Aided Diagnosis System for Microcalcification Cluster Detection in Digital Mammogram

T.Balakumaran
Electronics and Communication Engineering
Coimbatore Institute of Technology
Coimbatore

Dr.ILA.Vennila
Electrical and Electronics Engineering
PSG College of Technology
Coimbatore

ABSTRACT
Mammography is the most efficient method for breast cancer early detection. Clusters of microcalcifications are the sign of breast cancer and their early detection is the key to improve breast cancer prognosis. Microcalcifications appear in mammogram as tiny granular points, which are difficult to observe by radiologists due to their small size. An efficient method for automatic and accurate detection of clustered microcalcifications in digitized mammograms is the use of Computer Aided Diagnosis (CAD) systems. This paper presents a novel approach based on multiscale products of eigenvalues of Hessian matrix. The detection of microcalcifications is achieved by decomposing the mammograms by filter bank based on Hessian matrix into different frequency sub-bands, suppressing the low-frequency subband, and finally reconstructing the subbands containing only significant high frequencies features. The significant features are obtained by multiscale products. Preliminary results indicate that the proposed scheme is better in suppressing the background and detecting the microcalcification clusters than any other detection methods.

Keywords
Computer Aided Diagnosis (CAD), Hessian matrix, Multiscale product, Microcalcification detection.

1. INTRODUCTION
Today, Breast cancer is the common type of cancer among women and comprises the second leading cause of mortality after lung cancer. According to WHO report, more than 9 million women die due to breast cancer in worldwide every year. The earlier stage of the breast cancer is detected, the chance that a proper treatment can be prescribed.

A widely-used technique for breast cancer detection is the analysis of the Screening mammography [1]. Therefore, routine screening of mammogram programs are used to detect the earlier sign of cancer. The earliest sign of breast cancer is microcalcification, which is nodular in structure and varies in dimension from 0.6 mm to 2 mm. A detection of microcalcification in such earlier stage increases the probability of surviving [2]. Microcalcifications are approximately nodular, but the shape might be blob, elliptical and circular. The sensitivity of radiologists for microcalcification detection is 70% - 90% [3,4].

Therefore, computerized approach for breast cancer detection on mammogram has been developed. A Computer Aided Diagnosis (CAD) system is vital to increase the accuracy of the detection process [5-9]. The regions which are detected by CAD system then be observed by a radiologist, who finally confirms those as true or false positives. So the goal of a CAD system is to increase the accuracy of detection process.

In the past two decades, numerous methods have been proposed for breast cancer detection. These methods are based on suppressing background information and amplifying suspicious areas. Normally microcalcification appears as group of tiny bright spots in the mammograms. These bright spots correspond to high-frequency in the frequency spectrum. These high-frequency features of an image can be recovered using the wavelet-based subband decomposition. Most of the researchers have developed a method based on wavelet transform, which is a robust tool for image denoising, enhancement and image analysis [10], [11]. Wavelet transform is a powerful method for analyzing spatial-frequency phenomena and it allows the decomposition of image into different frequency bands without affecting the spatial locality.

Wang and Karayiannis [12], Strickland *et al. [13],* Yoshida *et al.* [14], [15] used a discrete wavelet transform, D.Sersic *et al.* [16] presented novel filter bank based on redundant wavelet transform, Laine *et al.* [17], [18] applied dyadic wavelet transform, Chun-Ming Chan *et al.* [19] developed an algorithm relying on multiscale wavelet analysis for detection of microcalcification. In their approach, mammogram is decomposed into different frequency subbands, the low frequency subband is suppressed and only the high frequency subbands are reconstructed. These high frequency subbands are enhanced by gain factors before reconstructing. The gain factors are determined by training, supervised learning and trial and error method. The resultant reconstructed image enhances not only microcalcification clusters but also some other structures, which are high frequency in nature. So enhancing only the microcalcification clusters is a challenging task in the detection process. To extract microcalcification clusters from high frequency subbands can be done based on analysis of the structure and size of the microcalcification clusters. The Hessian matrix is used to extract the different structures of object in medical imaging. Y.Sato *et al.* [20] used 3D Hessian matrix to classify the different structure of tissues in three-dimensional images. Frangi *et al.* [21] employed the Hessian matrix for vessel enhancement. Krissian *et al.* [22] developed a multi-scale detection in 3D images to detect the blood vessels. Nodular Structures in the image can be identified by using eigenvalues of Hessian matrix and dimension can be identified by multiscale analysis. The aim of our proposed method is to achieve early calcification detection. We have developed a CAD system to detect the calcifications of various dimensions based on eigenvalues of Hessian matrix.

The rest of the paper is organized as follows. Section 2 presents the microcalcification detection by proposed method. Section 3 presents experimental results and conclusion as last section.

2. PROPOSED METHOD

2.1 ROI Detection

In the first stage, Regions of Interest (ROIs) are detected in the mammogram image. We have proposed the multiresolution based histogram technique for the distinction between microcalcification cluster regions and normal regions in mammograms. The mammogram image is decomposed into four subimages by an undecimated wavelet transform (filter bank implementation without downsampling). Suspicious areas are found to be mainly concentrated in the detailed subimage. The size of each subimage is the same as the original image. The resulting horizontal detailed subimage is used to identify the region encircling the microcalcification clusters.

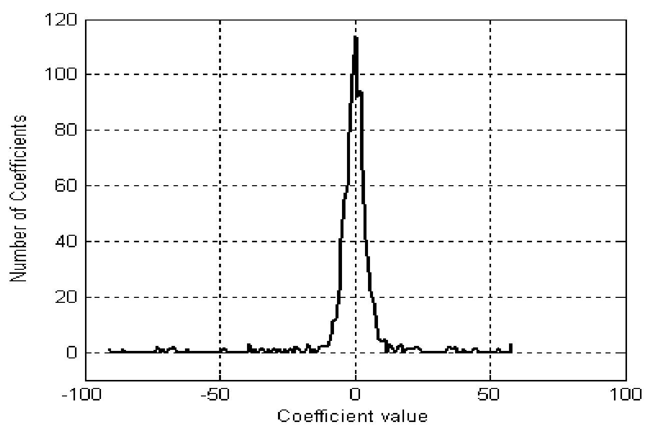

Fig. 1(a). Histogram of region with microcalcifications

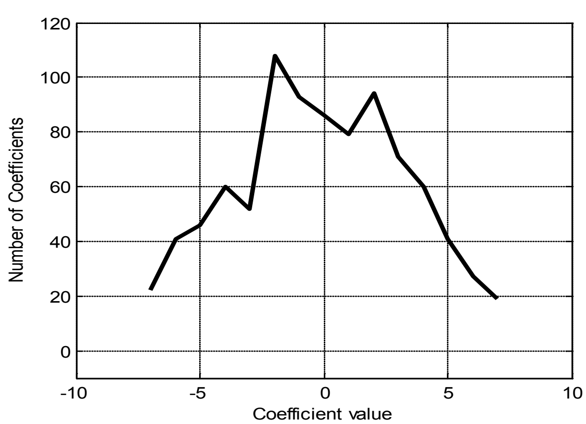

Fig. 1(b). Histogram of region without microcalcifications

The two different types of region with size of 30 x 30 were selected from the horizontal detailed subimage for simulation. An abnormal region was selected that contains the microcalcification clusters and a normal region that does not contain microcalcification clusters was selected randomly in mammogram. We determined the histogram of these two types of region. Fig. 1(a) shows the histogram of abnormal region and Fig. 1(b) shows the histogram of normal region. The histogram of region with microcalcification clusters has high positive tail and asymmetric. The distribution of right hand tail is larger than left hand tail.

The histogram of abnormal region is asymmetric and normal region is symmetric. Therefore, Abnormal ROIs can be identified by the difference between the absolute value of maximum positive coefficient and absolute value of maximum negative coefficient , third order moment (skewness) and fourth order moment (kurtosis).

Abnormal ROI detection is done as follows. Initially, mammogram image is decomposed by undecimated wavelet transform. In resulting horizontal detailed subimage was divided into 30 x 30 overlapping square blocks. The difference between the maximum positive coefficient (D^{+}_{max}) and maximum negative coefficient (D^{-}_{max}), third order moment and fourth order moment are calculated at each overlapping region.

The Difference value is computed by

$$D^{SR} = \left|D^{+}_{\max}\right| - \left|D^{-}_{\max}\right| \tag{1}$$

An estimate of the skewness and kurtosis is given by

$$S_k = \frac{\sum_{i=1}^{N} (xi - \widetilde{m})^3}{(N-1)\sigma^3} \tag{2}$$

$$K_u = \frac{\sum_{i=1}^{N} (xi - \widetilde{m})^4}{(N-1)\sigma^4} - 3 \tag{3}$$

where x_i is the input data over N observations, $\widetilde{m}$ is the ensemble average of x_i and σ its standard deviation.

The regions having difference value(D^{SR}) greater than 5, skewness value greater than 0.2 and kurtosis value greater than 4 is marked as region of interest (ROI). A 100x100 square matrix is chosen as the abnormal ROI size so that the microcalcification clusters center would be coincident with the ROI center and ROIs are extracted from the mammogram image.

2.2 Hessian matrix

After detecting abnormal ROIs from mammogram, the next stage is to pass ROI image through a multiscale filter bank, which was designed based on Hessian matrix. The Hessian matrix is a square matrix of second order partial derivates of an arbitrary function [23]. The second order partial derivatives are calculated as intensity difference around the pixel.

The Hessian matrix of function *S* is given by

$$H = \begin{bmatrix} \frac{\partial^2 S}{\partial x^2} & \frac{\partial^2 S}{\partial x \partial y} \\ \frac{\partial^2 S}{\partial y \partial x} & \frac{\partial^2 S}{\partial y^2} \end{bmatrix} \quad (4)$$

$\frac{\partial^2 S}{\partial x^2}$ is second order partial derivative in horizontal direction, $\frac{\partial^2 S}{\partial y^2}$ is second order partial derivative in vertical direction, $\frac{\partial^2 S}{\partial x \partial y}$ is first order partial derivative in horizontal followed by vertical direction and $\frac{\partial^2 S}{\partial y \partial x}$ is first order partial derivative in vertical followed by horizontal direction. Also it is symmetric matrix; the second order partial derivative $\frac{\partial^2 S}{\partial y \partial x}$ is the same as $\frac{\partial^2 S}{\partial x \partial y}$.

The eigenvalues of Hessian matrix provide the structure information of the image and this values state the local intensity variation in the direction of the associated eigenvectors v_1 and v_2.

The eigenvalues(λ_1,λ_2) are computed by

$$v_1^T H v_2 = diag[\lambda_1, \lambda_2] \quad (5)$$

The eigenvalues of Hessian matrix is more sensible to noise, it is essential to remove noise in the image without modifying the structure of microcalcifications. Frangi *et al.*[21] used Gaussian kernel to smooth out noise , we used smoothing filter to weaken the noise.

The first order derivative and averaging of a function *S* is given by

$$\frac{\partial S}{\partial x} = \frac{1}{2}(S(x) - S(x-1)) \quad (6)$$

$$\int S(x)dx = \frac{1}{2}(S(x) + S(x-1)) \quad (7)$$

The second order derivative and averaging of a function *S* is given by

$$\frac{\partial^2 S}{\partial x^2} = \frac{1}{4}(S(x+1) + S(x-1) - 2S(x)) \quad (8)$$

$$\int\int S(x)dxdx = \frac{1}{4}(S(x+1) + S(x-1) + 2S(x)) \quad (9)$$

To design two dimensional filter bank for computing Hessian matrix, initially one dimensional two channel filter bank is analysed is shown in Fig. 2.

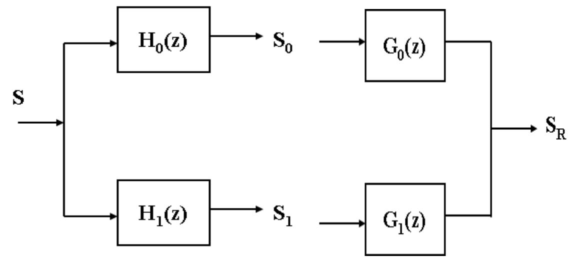

Fig. 2: One dimensional filter bank

S is an input signal and S_R is perfect reconstructed signal. The condition for perfect reconstruction is[24]

$$G_0(z)\, H_0(z) + G_1(z)\, H_1(z) = 1 \quad (10)$$

$H_0(z)$,$H_1(z)$ are analysis filter and $G_0(z)$, $G_1(z)$ are synthesis filters. Synthesis filter banks were designed to cancel the aliasing effect. The synthesis filter banks for perfect construction[24] are given by

$$G_0(z) = H_0(z),\ G_1(z) = -H_1(z) \quad (11)$$

$H_0(z)$ is the first order smoothing filter and $H_1(z)$ is the first order derivative filter. According to equation(6-7), the $H_0(z)$ and $H_1(z)$ is given by

$$H_0(z) = \frac{1}{2}(1 + z^{-1}) \quad (12)$$

$$H_1(z) = \frac{1}{2}(1 - z^{-1}) \quad (13)$$

The Second order partial derivative filter and averaging filter according to equation(8-9) is given by

$$H_0(z)\, H_0(z) = \frac{1}{4}(z^1 + z^{-1} + 2) \quad (14)$$

$$H_1(z)\, H_1(z) = \frac{1}{4}(z^1 + z^{-1} - 2) \quad (15)$$

Figure 3 shows the two dimensional filter bank, some of the filters were moved from synthesis to analysis and vice versa to compute the Hessian matrix and it is shown in Fig.4. Fig.5 is equivalent to Fig.4 according to equation(11). The multiscale image analysis is achieved by approximation subimage S_jf is iterated to number of scales. Figure 6 shows iterated multiscale filter, image is smoothed and dilutes the noise at each scale. The filter $H_0(z^j)$ and $H_1(z^j)$ is 2^j scale dilation of $H_0(z)$ and $H_1(z)$. The $\frac{\partial^2 S}{\partial x^2}$, $\frac{\partial^2 S}{\partial y^2}$, $\frac{\partial^2 S}{\partial x \partial y}$ are corresponds to W_j^V , W_j^H and W_j^D.

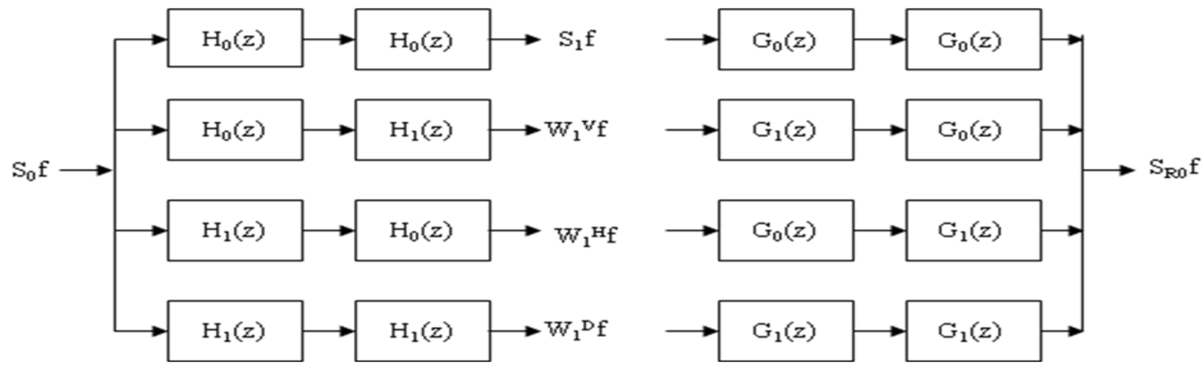

Fig. 3: Two dimensional filter bank

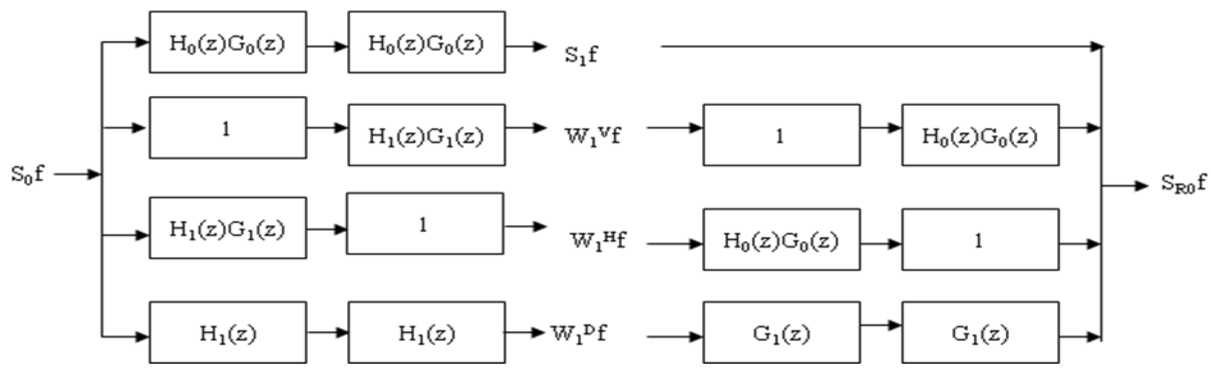

Fig. 4: Alteration of two dimensional filter bank for calculating Hessian matrix

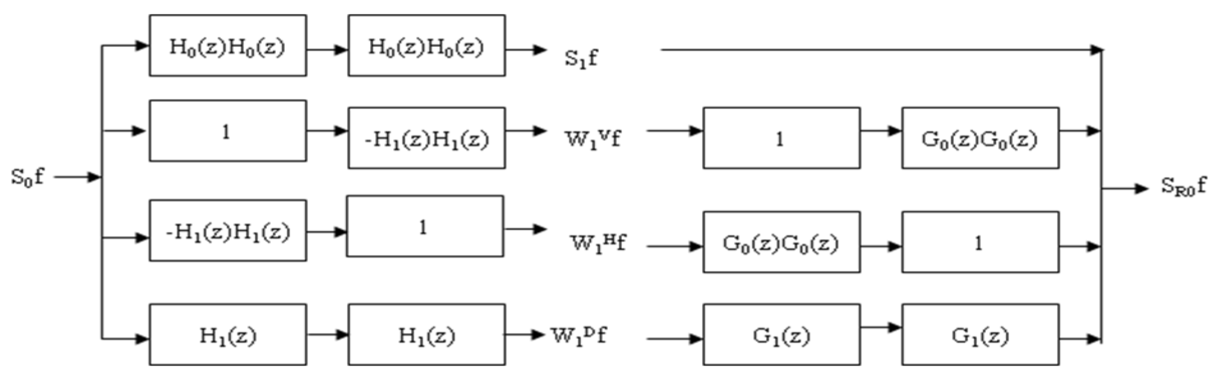

Fig. 5: Filter bank designed based on Hessian matrix which is equivalent to Fig. 4

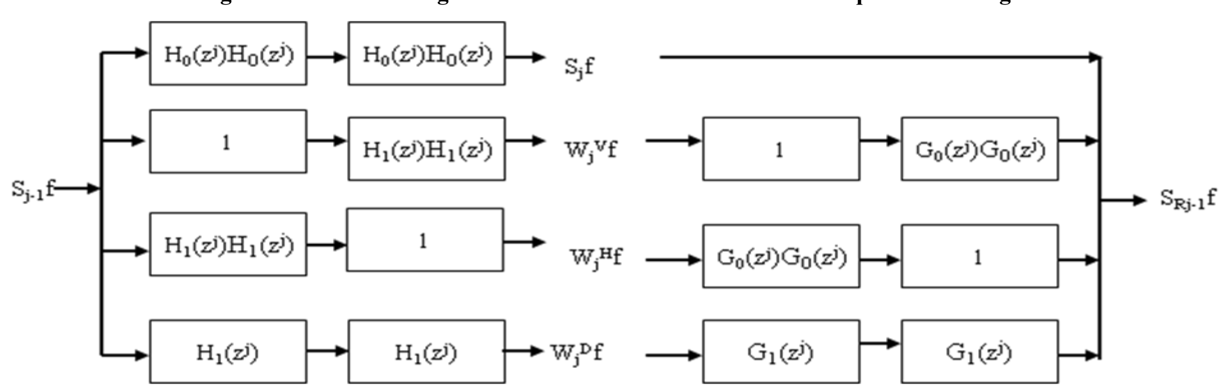

Fig. 6: Hessian matrix filter bank with iterating low pass image

2.3 Multiscale Product Analysis

In order to study the relation between eigenvalues of Hessian matrix with microcalcification clusters, we have taken a microcalcification profile from mammogram and tested.

A single row on mammogram image was taken, which contains microcalcification cluster. Figure 7(b) shows the line of image, the sharp peaks indicate microcalcification cluster and other values indicate unwanted artifacts and background. Fig. 7(c-e) and Fig. 7(f-h) show two eigenvalues of Hessian matrix for this line at different scales. Multiscale analysis was applied to line of image, where scale increases the eigenvalues of calcifications are reduced.

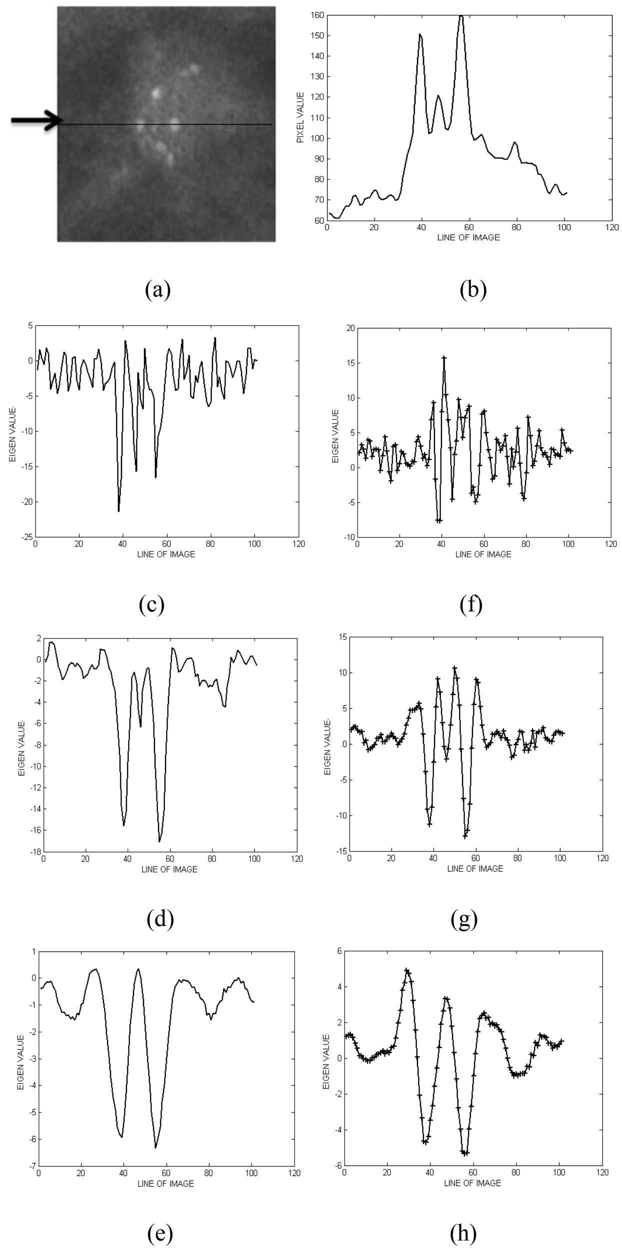

Fig. 7. (a) Region with microcalcifications clusters (b) The line on image (c-e) eigenvalues(λ_1) from scale 1 to 3 (f-h) eigenvalues(λ_2) from scale 1 to 3

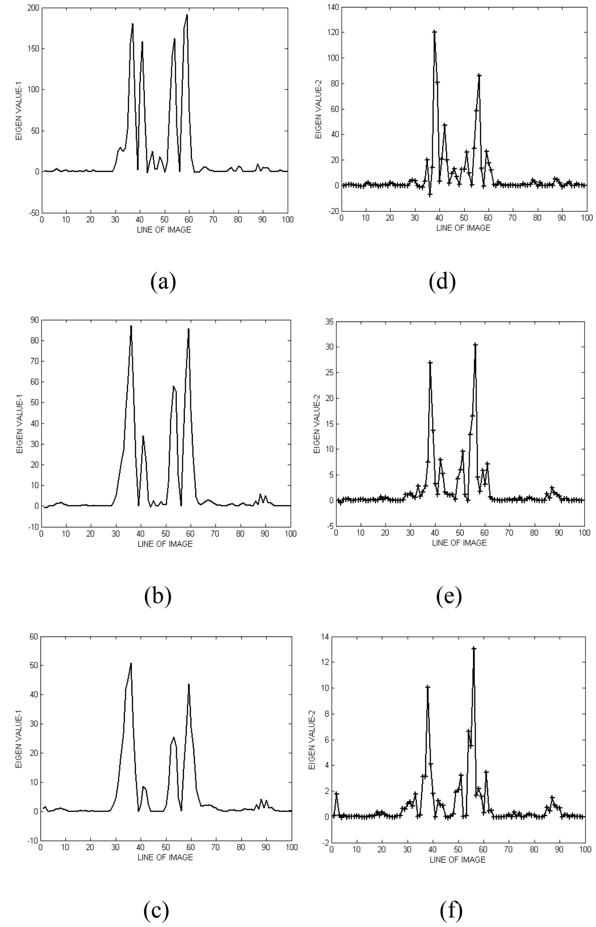

Fig. 8. (a-c) Multiscale products of eigenvalues(λ_1) (d-f) Multiscale products of eigenvalues(λ_2)

Notice that the eigenvalues of calcifications have high magnitude value(negative) across scales while non-specific background has low values. It is complicated to pick up the calcifications because eigenvalues of calcifications are surrounded by insignificant neighborhood values. To avoid this problem, we present multi-scale product scheme to incorporate the merits of interscale dependencies for microcalcification detection. In the Multiscale products, calcifications can be efficiently distinguished from non-relevant ones. Multiscale products are calculated by multiplying adjacent scale of eigenvalues. These products are used to increase the magnitude of the calcifications and to weaken the homogeneous region. Fig. 8 shows multiscale product of eigenvalues at adjacent scales. Indeed, it is easy to extract the singularity (microcalcification) in the the mammogram.

The multiscale products of eigenvalues are calculated by

$$P_{1,j} = \lambda_1^{\ j} . \lambda_1^{\ j+1} \tag{16}$$

$$P_{2,j} = \lambda_2^{\ j} . \lambda_2^{\ j+1} \tag{17}$$

Where λ^j, λ^{j+1} are eigenvalues of Hessian matrix at scale j and $j+1$. The multiscale products for two eigenvalues (λ_1, λ_2) are calculated, based on this products thresholding is applied to extract the calcifications.

The algorithm is summarized as follows. An iterated filter bank based on Hessian matrix(Fig.6) is applied to mammogram, which is decomposed into different frequency subbands. The eigenvalues of Hessian matrix at each subband are computed. Two adjacent eigenvalues of subbands are multiplied and thresolding is applied to the multiscale products.

The detail coefficients are threshold by

$$W_j^M(x,y) = \begin{cases} W_j^M(x,y) & P_{k,j}^M \geq \lambda . Max(P_{k,j}^M), k = 1,2 \\ 0 & otherwise \end{cases} \quad (18)$$

Where λ is the bias thresholding value in the range of 0.1 to 0.3 and $Max(P_{k,j}^M)$ is the maximum value of multiscale product at each subband. Where M is the variable used to indicate the horizontal, vertical and diagonal subbands. Finally, suppressing the coarsest approximation subband, and reconstructing only the detail subbands. The multiscale product technique is used to distinguish the calcifications against background effectively.

3. EXPERIMENTAL RESULTS

The proposed approach was tested in MATLAB 10.0 and verified on the set of mammogram image with different features. The set of mammogram were obtained from DDSM database and resolution of a mammogram is 50 µm/pixel and gray level depths are 12 bits. The first step of microcalcification detection is to find the abnormal regions, which are identified by multiresolution based histogram technique. Fig. 9(a) shows a part of mammogram image with microcalcification clusters and Fig. 9(b) shows suspicious areas are marked by white and normal regions are marked by black.

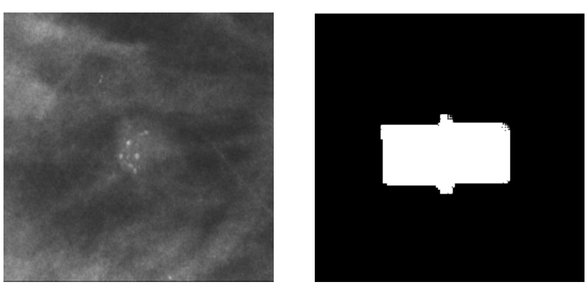

(a) (b)

Fig. 9: ROI detection (a) Part of mammogram with microcalcification clusters (b) suspicious ROI detection

In the next stage, the microcalcification clusters are detected by proposed filter bank based on Hessian matrix. The performance of our proposed method was compared with background suppressed algorithm. For convenience, we compared microcalcification detection by 2D wavelet transform [12] and multiscale wavelet method[19].

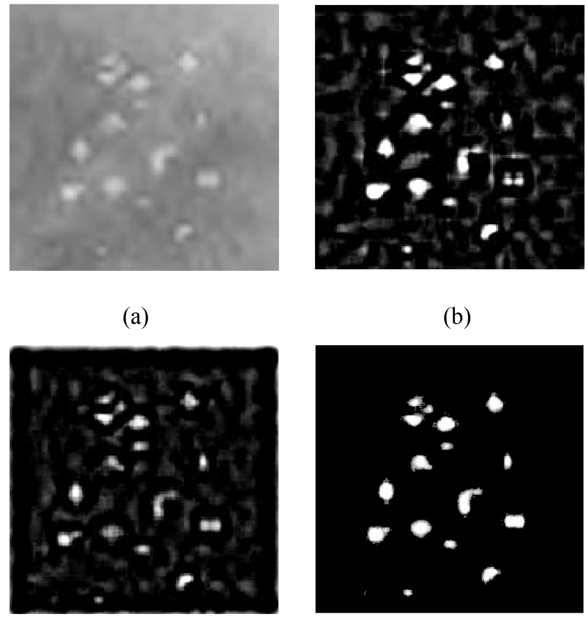

(a) (b)

(c) (d)

Fig. 11 : Detection of microcalcification (a) Abnormal ROI (b) Detection by 2D WT (c) Detection by Multiscale WT (d) Detection by Proposed Method

Fig.11(a) shows an abnormal region which contains microcalcification clusters and Fig.11(b-d) shows microcalcification detection by 2D wavelet, multiscale wavelet and proposed method. It is found from the results, microcalcification clusters are detected accurately and the other structures are suppressed by proposed method. The detection result obtained by the proposed method seems to be the most suitable, since it identifies the location of microcalcifications. The detection capability of the proposed method is much higher than the 2D wavelet method and multiscale wavelet method.

4. CONCLUSION

The development of a CAD system for automatic detection of microcalcification clusters in mammogram was presented. Microcalcification cluster detection based on wavelet decomposition is used in many works before. In this paper, detection by filter bank which was designed based on Hessian matrix. In many conventional methods, detection of microcalcifications is achieved by suppressing low-frequency subband and reconstructing all high frequency subbands. In our proposed scheme, reconstructing the high frequencies contains only microcalcification clusters. This method is better to differentiate the microcalcification clusters from insignificant tissues. The computational complexity of the proposed algorithm is high compared to 2D wavelet transform. But the results are promising that this method could detect the microcalcifications accurately than 2D wavelet transform. The proposed algorithm was tested on both normal and abnormal images. We tested 88 images taken from DDSM mammogram database. Based on the results, the proposed method detects the microcalcifications up to 97.8% accuracy.

5. ACKNOWLEDGMENTS
The authors would like to thank Dr.A.Murugesan, Radiologist, Johnsons MRI Scan Centre & Diagnostic Centre**,** Erode for providing us with sufficient data and his valuable advice.

6. REFERENCES
[1] Heath, M., Bowyer, K., Kopans, D., Moore, R., Kegelmeyer, P . 2000. The digital database for screening mammography. In: The Proceedings of the 5th International Workshop on Digital Mammography. Medical Physics Publishing(Madison,WI), pp.662–671.

[2] C. J. Vyborny and R. A. Schmidt. 1994. Technical image quality and the visibility of mammographic detail, in Syllabus: A Categorical Course in Physics-Technical Aspects of Breast Imaging, A. G. Haus and M. J. Yaffe, Eds. Oak Book III: Radiological Society of North America, pp.103–111.

[3] G. M. te Brake and N. Karssemeijer .1999. Single and multiscale detection of masses in digital mammograms.IEEE Trans. Medical Imaging, vol. 18, no. 7, pp. 628–639.

[4] R. G. Bird, T. W. Wallace, and B. C. Yankaskas .1992. Analysis of cancers missed at screening mammography. Radiology,vol. 184, pp. 613–617.

[5] M. L. Giger, P. Lu, Z. Huo, U. Bick, C. J. Vyborny, R. A. Schmidt, W. Zheng, C. E. Metz, D. Wolverton, R. M.Nishikawa, W. Zouras, and K. Doi .1994. CAD in digital mammography: Computerized detection and classification of masses. in Digital Mammography, A. G. Gale, Ed. et al. Amsterdam/New York: Elsevier Science, pp. 281–287.

[6] W. P. Kegelmeyer, Jr, J. Prundeda, P. Bourland, A. Hillis, M. Riggs, and M.Nipper . 1994. Computer aided mammographic screening for Speculated lesions. Radiology, vol. 191, pp. 331–337.

[7] K. Doi, H. MacMahon, S. Katsuragawa, R. M. Nishikawa, and Y. Jiang . 1999. Computer-aided diagnosis in radiology: Potential and pitfall. Eur. J. Radiol., vol. 31, pp. 97–109.

[8] H. Li, K. J. Liu, and S. Lo . 1997. Fractal modeling and segmentation for the enhancement of microcalcifications in digital mammograms. IEEE Trans.Med. Imag., vol. 16, no. 6, pp. 785–798.

[9] S. Yu, L. Guan .1998. A CAD system for the automatic detection of clustered microcalcifications in digitized mammogram films", IEEE Trans.Med. Imag., vol. 19, no.2, pp. 115–126,1998

[10] S.Mallat . 1987. A compact multiresolution representation: the wavelet model. Proc. IEEE Computer Society Workshop on Computer Vision, IEEE Computer Society Press, Washington, D.C., p.2-7.

[11] S. Mallat .1989. Multifrequency channel decompositions of images and wavelet models, IEEE Trans. Acoust. Speech Signal Process., vol. 37, no. 12, pp. 2091–2110.

[12] Ted C. Wang and Nicolaos B. Karayiannis .1998. Detection of Microcalcifications in Digital Mammograms Using Wavelets. IEEE Tran. on Medical Imaging, vol. 17, pp. 498-509.

[13] R. N. Strickland and H. I. Hahn . 1996. Wavelet transform for detecting microcalcifications in mammograms. IEEE Trans. Med. Imag., vol. 15, no. 2, pp. 218–229.

[14] H. Yoshida, K. Doi, and R. M. Nishikawa.1994. Automated detection of clustered Microcalcifications. Proc. SPIE (Digital Mammograms using Wavelet Transform Tech., Med. Imag. 1994: Image Process.), vol. 2167, pp. 868–886.

[15] H. Yoshida, K. Doi, R. M. Nishikawa, M. L. Giger, and R. A. Schmidt. 1996. An improved computer-assisted diagnostic scheme using wavelet transform for detecting clustered microcalcifications in digital mammograms. Acad. Radiol., vol. 3, pp. 621–627.

[16] Damir Sersic and Sven Loncaric..1998. Enhancement of Mammographic Images for Detection of Microcalcifications. Fac. of Electrical Engineering and Computing, Zagreb, Croatia.

[17] A.F. Laine, S. Schuler, J. Fan, and W. Huda. 1994. Mammographic feature enhancement by multiscale analysis. IEEE Trans. Med. Imag., vol. 13,no. 4, pp. 725–740.

[18] A.F. Laine, J. Fan, andW. Yang. 1995. Wavelets for contrast enhancement of digital mammography. IEEE Eng. Med. Biol. Mag.,vol. 14, no.5, pp. 536–550.

[19] Chun-Ming Chang and Andrew Laine. 1999. Coherence Of Multiscale Features for Enhancement of Digital Mammograms. IEEE Tran. on Information Technology in Biomedical, vol. 3, pp. 32-46.

[20] Y. Sato, C.-F. Westin, A. Bhalerao, S. Nakajima,N.Shiraga, S. Yoshida, and R. Kikinis .2000. Tissue classification based on 3D local intensity structures for volume rendering. IEEE Transactions on Visualization and Computer Graphics, 6(2):160–180.

[21] Frangi, W. Niessen, K. Vincken, and M. Viergever. 1998. Multiscale vessel enhancement filtering. Medical Image Computing and Computer - Assisted Intervention – MICCAI'98,(1496):130–137.

[22] K. Krissian, G. Malandain, N. Ayache, R. Vaillant, and Y.Trousset . 2000. Model based detection of tubular structures in 3D images. Comp. Vision and Image Understanding, vol. 80, no. 2, pp. 130-171, November 2000

[23] Sato Yoshinobu, et al.: 3D Multi-Scale Line Filter for Segmentation and Visualization of Curvilinear Structures in Medical Images, in proc. of the First Joint Conference on Computer Vision, Virtual Reality and Robotics in Medicine and Medial Robotics and Computer-Assisted Surgery, vol 1205 of Lecture Notes in Computer Science, pages 213–222, Mar. 1997

[24] D.Esteban, C.Galand :1977. Application of Quadrature mirror filter to split Band Voice Coding Schemes. Proc. IEEE ICASSP'77,pp.191-195.